

Electrode biasing experiments in the J-TEXT tokamak

Y. Sun, Z. P. Chen*, T. Z. Zhu, H. Liu, X. Ke, G. Zhuang

State Key Laboratory of Advanced Electromagnetic Engineering and Technology, Huazhong

University of Science and Technology, Wuhan Hubei, 430074, China

Introduction

For decades, biasing experiments have been carried out on many devices with different magnetic configurations [1-4]. The most common phenomenon obtained was the enhancement of local $E \times B$ shear flows, accompanied with suppression of turbulence and improvement of global confinement [5]. A newly designed electrode biasing system (EBS) has been constructed and performed experimentally in the J-TEXT tokamak ($R = 105$ cm, $a = 26.5$ cm) [6] recently. The influence of both positive and negative bias on global and plasma-edge parameters has been comparatively studied.

Experimental set-up

The schematic of electrode biasing system (EBS) is shown in figure 1 (a). To reduce the influence on the plasma, the system is designed to contain a pneumatic driving part, and thus the electrode can reciprocate in a single discharge. The preliminary biasing experiments were executed in hydrogen discharges with limiter configuration. The discharge parameters were set as follows: the plasma current $I_p = 120$ kA, the toroidal magnetic field $B_t = 1.8$ T, and the central line-averaged density $\langle n_e \rangle = (1.5 \sim 2.2) \times 10^{19} \text{ m}^{-3}$. During a discharge, a disk shaped (1 cm thick and 4 cm in diameter) electrode head, which is made of hard graphite, was inserted radially into the plasma and reached about 4 cm inside limiter. The bias voltage applied during the flat-top phase of plasma current was in the range of $-300 \sim 300$ V, and the duration of biasing was set as 150 ms. A reciprocating probe system equipped with a Langmuir four-tip probe has been used to monitor the edge plasma

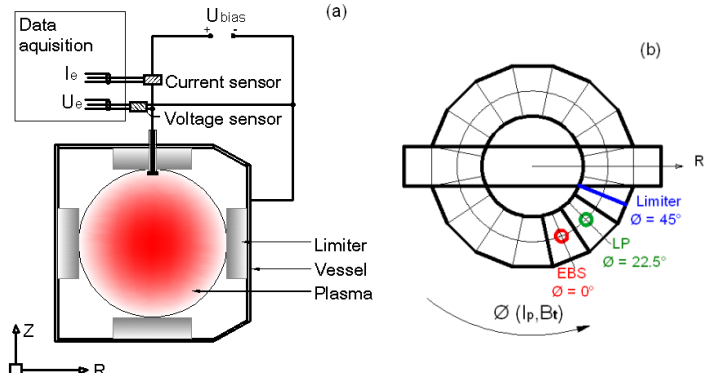


Figure 1. Schematics of (a) electrode bias system (EBS) and (b) the arrangement of the Langmuir probe (LP) system and EBS.

behavior in the experiment [7]. As shown in figure 1 (b), both the LP system and EBS are installed on the top ports of J-TEXT, and at toroidal degrees of 22.5 ° and 45 ° from the limiter, respectively.

Experimental results

Figure 2 shows the evolutions of global parameters under three different bias conditions, including 0V bias (shot # 1027591), +300V bias (shot # 1027589) and -300V bias (shot # 1027594). In the bias phase (0.28 ~ 0.43 s), the electrode current I_{bias} drawn under +300V bias is in the range 60 ~ 100 A, which is larger than the -300V bias case where $I_{\text{bias}} = 20 \sim 70$ A, as expected. The global confinement is improved under both polarity bias cases, with increments of central line averaged density and soft X-ray emission as well as reduction of edge H_{α} radiation. The profiles provided below are obtained from the probe data during the inserting phase 0.33 ~ 0.37 s, as shown in figure 2 (f).

The influences of bias on edge parameters are more significant. Comparing to the 0V bias case, both the absolute value and shearing rate of E_r are obviously increased under bias with both polarities (figure 3 (b)). Under positive bias, E_r has a maximum value about 8.6 kV/m with the averaged shearing rate as $\sim 2.4 \times 10^5$ s⁻¹ in the broad shear layer ($\Delta r = -2.0 \sim 1.5$ cm). While under negative bias, the maximum amplitude of E_r is ~ -4 kV/m, with the mean shearing rate in the shear layer ($\Delta r = -2.0 \sim 1.5$ cm) as 1.1×10^5 s⁻¹. Comparatively, the shearing rate for the 0V bias case is as weak as about 0.5×10^5 s⁻¹ at the vicinity of limiter. The modification of the fluctuations of plasma-edge parameters is found to be sensitive to the polarities of bias. The amplitude of V_f fluctuation increases greatly under positive bias at the vicinity of limiter,

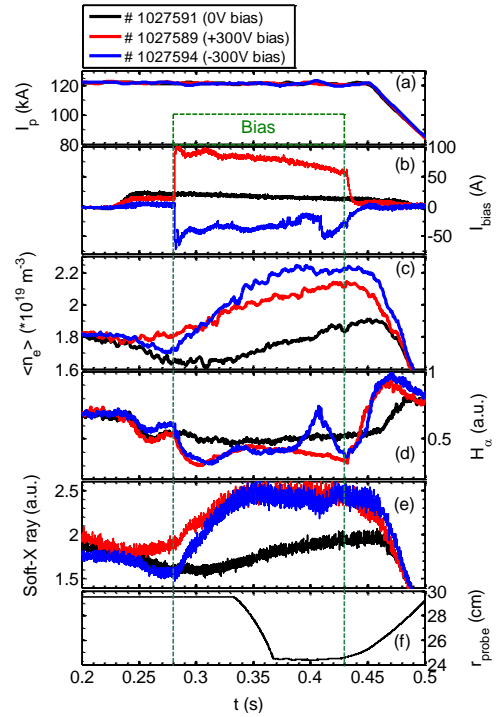


Figure 2. Evolutions of (a) plasma current, (b) electrode current, (c) central line-averaged density, (d) edge H_{α} radiation, (e) soft-X ray emission and (f) trace of Langmuir probe.

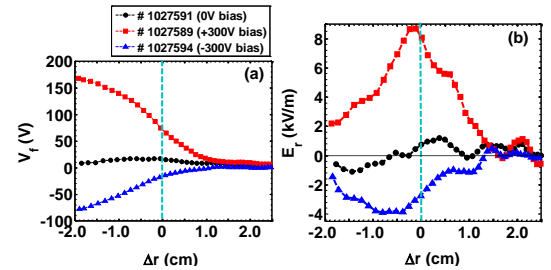


Figure 3. Equilibrium profiles of (a) floating potential V_f and (b) radial electric field E_r under different bias cases at plasma-edge.

while decreases under negative bias, comparing to the 0V bias case (figure 4 (a)). Ignoring the contribution of electron temperature, the level of turbulent particle flux is determined by the amplitudes of I_s and E_θ fluctuations, their coherence γ_{IE} and phase shift θ_{IE} as:

$$\Gamma_r \approx \langle \tilde{I}_s \cdot \tilde{E}_\theta \rangle / B_r = \sqrt{\langle \tilde{I}_s^2 \rangle \cdot \langle \tilde{E}_\theta^2 \rangle} \cdot \gamma_{IE} \cdot \cos(\theta_{IE}) / B_r.$$

As shown in figure 4 (b) ~ (f), the reduction of turbulent particle flux is only due to the suppression of fluctuation levels under positive bias. For the negative bias case, the suppression of turbulent particle flux is attributed to the combined role of fluctuations suppression and de-phasing inside limiter.

Figure 5 shows the local wavenumber frequency spectrum estimated at $\Delta r = -2$ cm based on the two point spectral analysis technique [8]. The positive k_θ indicates the ion diamagnetic drift (IDD) direction, while the negative one indicates the electron diamagnetic drift (EDD) direction. Under negative bias, the local turbulence propagates towards EDD. Under positive bias, the distribution of spectral power density shows a clear turning point at around 15 kHz, as marked in figure 5 (b). In the frequency range below 15 kHz, the wavenumber k_θ keeps close to 0 cm^{-1} , with the power density peaks at $f \sim 12$ kHz. While in the frequency range above 15 kHz, the spectral power density locates in the positive wavenumber region in an approximate linear way. The 12 kHz low-frequency mode (LFM)

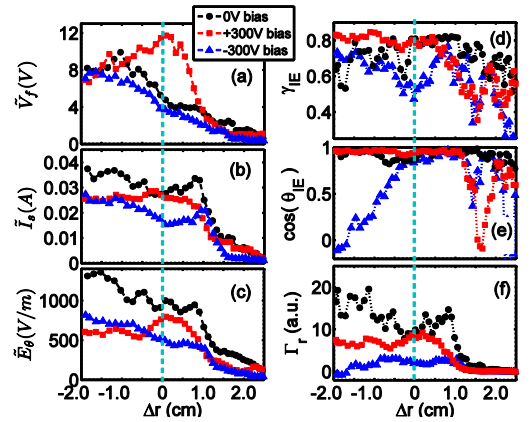


Figure 4. Profiles of fluctuations for floating potential (a), ion saturation current (b), poloidal electric field (c), the coherence (d) and cross-phase (e) of I_s and E_θ fluctuations and turbulent particle flux (f) under different bias cases.

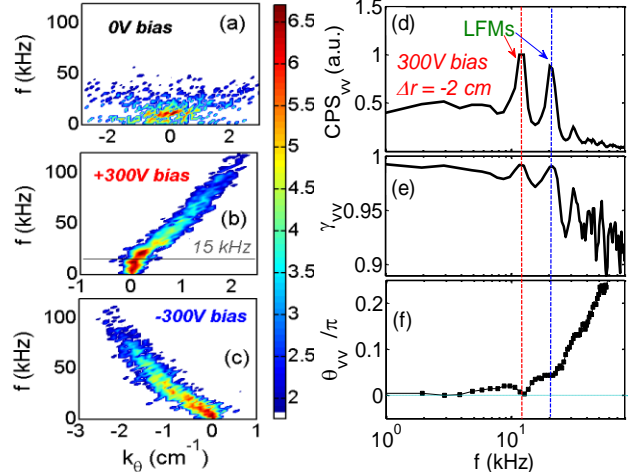


Figure 5. Frequency-wavenumber spectra $S(k_\theta, f)$ ((a) ~ (c)), as well as cross power spectra (d), coherence (e) and phase shift spectra (f) of two poloidally separated floating potentials at $\Delta r = -2$ cm, under +300V bias cases.

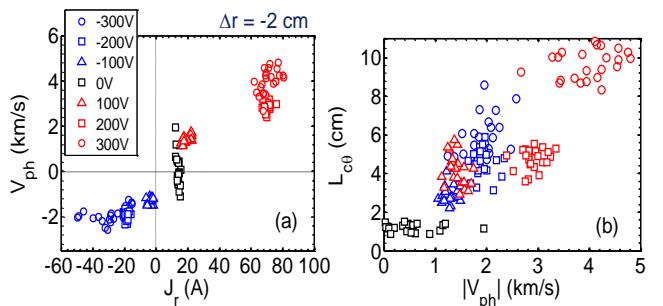


Figure 6. Distributions of V_{ph} measured at $\Delta r = -2$ cm as a function of radial current J_r (a), and poloidal correlation length L_{c0} as a function of absolute value of phase velocity V_{ph} (b) under different bias cases.

may corresponds to a geodesic acoustic mode (GAM), with extremely high coherence and near-zero cross-phase between fluctuations of 7 mm poloidally separated floating potentials (see figure 5 (d) ~ (f)).

The poloidal phase velocity of turbulence V_{ph} is modified greatly under bias, and shows a positive correlation with radial current drawn by the biased electrode, as shown in figure 6 (a). The phase velocity is towards to EDD direction under negative bias and reverses to IDD direction under positive bias. And this statistical result demonstrates the role of $J_r \times B$ torque in driving poloidal rotation of local plasma. The poloidal correlation length is also increased dramatically under bias, and shows a positive correlation with the amplitude of poloidal phase velocity, as presented in figure 6 (b).

Summary

The influence of both positive and negative bias on global and plasma-edge parameters has been comparatively studied. The improvement of global confinement and the suppression of plasma-edge turbulent particle transport are clearly observed under bias with both polarities. The poloidal correlation length of turbulence is increased greatly under bias, and shows a positive correlation with the amplitude of poloidal phase velocity.

Acknowledgement

This work is supported by National Natural Science Foundation of China (No. 10935004 and 10990214) and the Ministry of Science and Technology (Contract No.2011GB109001, 2013GB106001).

References

- [1] Taylor R J, Brown M L, Fried B D, Grote H, Liberati J R, Morales G J, and Pribyl P 1989 *Phys. Rev. Lett.* **63** 2365
- [2] Weynants R R *et al* 1992 *Nucl. Fusion* **32** 837
- [3] Pedrosa M A, Silva C, Hidalgo C, Carreras B A, Orozco R O and Carralero D 2008 *Phys. Rev. Lett.* **100** 215003
- [4] Antoni V, Martines E, Desideri D, Fattorini L, Serianni G, Spolaore M, Tramontin L and Vianello N 2000 *Plasma Phys. Control. Fusion* **42** 83
- [5] Van Oost G *et al* 2003 *Plasma Phys. Control. Fusion* **45** 621
- [6] Zhuang G *et al* 2011 *Nucl. Fusion* **51** 094020
- [7] Chen Z P, Sun Y, Wang Z J, Yang Z J, Ding Y H and Zhuang G 2012 *Plasma Sci. Technol.* **14** 1041
- [8] Beall J M, Kim Y C and Powers E J 1982 *J. Appl. Phys.* **53** 3933